Physica B 404 (2009) 2898–2903

Contents lists available at ScienceDirect

Physica B

journal homepage: www.elsevier.com/locate/physb

Multiprobe high-pressure experiments in $CePd_{0.6}Rh_{0.4}$ and $CePd_3$

P. Pedrazzini [a,*], D. Jaccard [a], M. Deppe [b], C. Geibel [b], J.G. Sereni [c]

[a] DPMC, University of Geneva, 24 Quai Ernest-Ansermet, CH-1211 Geneva, Switzerland
[b] Max-Planck-Institute for Chemical Physics of Solids, Nöthnitzer Str. 40, 01187 Dresden, Germany
[c] Lab. Bajas Temperaturas, Centro Atómico Bariloche (CNEA), 8400 S.C. de Bariloche, Argentina

ARTICLE INFO

PACS:
72.15.Jf
75.30.Mb
75.40.Cx

Keywords:
Ce compounds
Ferromagnetism
Quantum phase transition
High pressure
Resistivity
Seebeck coefficient
Specific heat

ABSTRACT

Results of recent multiprobe high-pressure experiments on ferromagnetic $CePd_{0.6}Rh_{0.4}$ and intermediate-valent $CePd_3$ are presented. Simultaneous resistivity (ρ), thermopower (S), and ac heat capacity measurements show that the long-range ferromagnetic state of $CePd_{0.6}Rh_{0.4}$ vanishes in the proximity of a sharp valence-crossover pressure $p_V \approx 7.5$ GPa, i.e. before reaching a quantum critical point. However, a magnetic signal that is progressively suppressed is still detected at higher pressures. For $CePd_3$, the results of simultaneous $\rho(T,p)$ and $S(T,p)$ measurements up to 22 GPa and down to the mK temperature range show a surprisingly weak pressure dependence.

1. Introduction

Pressure is one of the fundamental control parameters in current research on strongly correlated electron systems (SCES). The difficulty of high-pressure experiments depends largely on the pressure range, the physical property under probe, and the control of other parameters like T or H. Two main concerns are, in any case, the hydrostaticity and the repeatability of pressure conditions. Considering these issues and taking into account the large sample-dependence of measured properties, high-pressure experiments probing several physical properties on a *single* sample on *exact* p-conditions are a desired breakthrough.

High-pressure studies [1] have shown that the ground state of magnetically ordered Ce-based systems evolve from magnetism to a non-magnetic state of heavy effective masses. Moreover, as the Kondo energy $k_B T_K$ increases further with p, actually surpassing the overall crystal-field splitting Δ_{CEF}, a new change of regime is observed, in which valence fluctuations between the Ce^{3+} and Ce^{4+} configurations dominate the physics of intermediate valence compounds (IVCs). Many fundamental questions concerning the succession of ground states are still open. Among them, major issues concern the magnetic instability region, the occurrence of quantum criticality, non-Fermi liquids, unconventional magnetism, and superconductivity, and the way the Fermi liquid establishes in the $p > p_c$ regime.

Recently, we have focused our interest on two problems: the (non)occurrence of ferromagnetic quantum criticality in Ce compounds [2] and the characteristics of the metallic phase existing away from the magnetic instability. We have thus selected to study two members of the Ce–Pd binary system [3]: ferromagnetic Rh-doped α-CePd, and intermediate-valent $CePd_3$. We present here the results of high-pressure multiprobe experiments performed on these systems.

2. Experimental: multiprobe measurements at high pressures

In the context of the Bridgman anvil high-pressure technique employed in our research, we define *multiprobe experiments* those intended to probe at least two physical properties simultaneously. These experiments require the basic capacity of introducing numerous electrical leads (typically 8+) within the sample space. Fig. 1 shows one of the several possible designs intended to measure the electrical resistivity, ρ, thermopower, S, and a.c. heat capacity, C, at high pressures, and their field dependence. By introducing small modifications to this configuration, it is not difficult to include the possibility of measuring Hall and Nernst signals with a field H applied perpendicular to a wider sample [4]. A key requirement to perform such measurements is the good control of the geometrical stability of the cell under pressure [5], that allows us to perform straightforward d.c. resistivity

* Corresponding author. Present address: Centro Atómico Bariloche (CNEA), 8400 S.C. de Bariloche, Argentina. Tel.: +54 2944 44 5137.
E-mail address: pedrazp@cab.cnea.gov.ar, Pablo.Pedrazzini@unige.ch (P. Pedrazzini).

0921-4526/$ - see front matter © 2009 Elsevier B.V. All rights reserved.
doi:10.1016/j.physb.2009.07.042

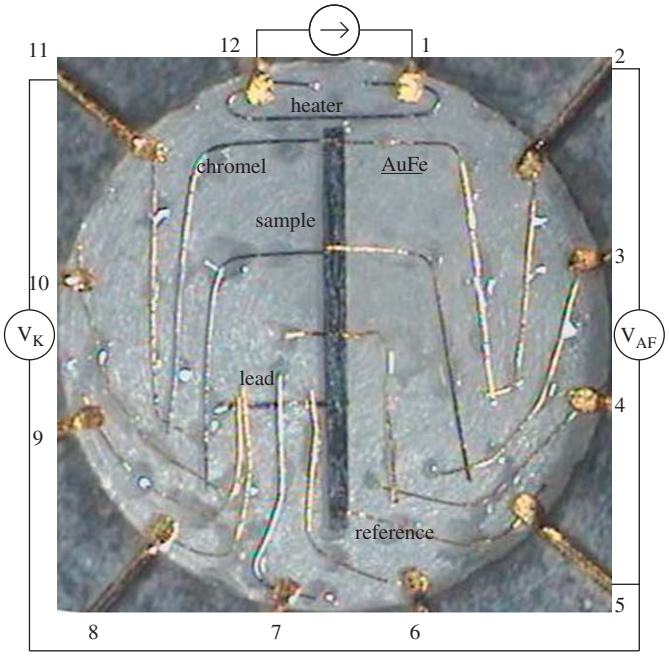

Fig. 1. Image of the high-pressure cell containing a $CePd_3$ sample. The pyrophyllite gasket (grey) and lower steatite-disk (white) have been positioned on top of atungsten–carbide (or sintered-diamond) lower Bridgman anvil. For pressurization a second steatite-disk is added. For further details see Ref. [5].

measurements. The geometrical factor $G(p)$ varies only weakly with pressure, and its main source of error is the measurement of the linear dimensions of the sample and contacts. It is interesting to note that the $\rho(300\,\mathrm{K}, p)$ of the Pb pressure-gauge measured in diverse pressure cells is reproducible within few percents.

Adding a resistive heater close to one extreme of the sample and carefully selecting thermocouple (TC) wires, typically Au, AuFe, and chromel in our application, permits to determine the low-T Seebeck coefficient [5,6]. The success of such approach relies on the fast decay of the temperature profile away from the heater, $T(x)\sim\exp(-x/\lambda)$ with $\lambda\sim100-200\,\mu\mathrm{m}$, that guarantees that the non-heated extreme of the sample keeps the T_0 temperature of the bath. The absolute thermopower of the sample can be deduced from the voltages V_K and V_{AF} measured between the chromel (wire 11) and AuFe [2] branches and [5], respectively. Small corrections related to the misplacement of the TC branches may be introduced. They are important when the thermopower S is large ($|S|\gg S_K - S_{AF}$), as in $CePd_3$ discussed in Section 4.

The inclusion of a second thermocouple further away from the heater has two main advantages. First, knowing the spacing between both TC, it is possible to introduce corrections to the measured $S(T)$. Second, it allows different options to estimate the heat capacity of the sample either by heating with the heater, the other thermocouple or the sample itself, especially when $\rho(T)$ changes only weakly with T [7,8].

In a solid medium like steatite, pressure inhomogeneity is typically of the order of $0.05-0.1p$. In many cases this spread is inadmissible and so, different research groups undertook the development of high-pressure techniques using liquid mediums. It is very difficult [9] to adapt the "ideal" medium, helium, to multiprobe experiments as described here. An interesting alternative is the adaptation of the Bridgman technique to liquid medium typically used in low-p piston-cylinder cells. Among different realizations of this idea [10,11], the setup of Ref. [11] is currently being employed to perform simultaneous $\rho(T)$ and $C(T)$ measurements down to very low temperatures.

3. Vanishing ferromagnetism and sharp valence crossover in pressurized $CePd_{0.6}Rh_{0.4}$

Ferromagnetic Ce compounds are far less abundant [12] than antiferromagnetic ones, in part a reason why the critical region of such systems has been scarcely studied. Orthorhombic CrB-type CePd displays a ferromagnetic ground state below $T_C = 6.5$ K. Its Curie temperature increases at low pressures at roughly $dT_C/dp\sim0.3$ K/GPa [13], hinting that CePd lies on the low-coupling side of Doniach diagram. This is confirmed by "chemical pressure" studies performed on the $CePd_{1-x}Ni_x$ alloy, showing that a maximum $T_C \approx 10.3$ K exists for $x \approx 0.5$ [14]. The Curie temperature $T_C(x)$ is found to drop steeply in a very narrow x-interval close to the CeNi limit ($x = 1$) [14,15], an indication that the magnetic transition may become first order. One arrives at a similar conclusion if the T_C dependence of isostructurals $CePt_{1-x}Ni_x$ [16] and pressurized CePt [17] are analyzed. These three examples illustrate what seems to be the general case for the (chemical) pressure suppression of ferromagnetism in Ce compounds: T_C ends at a finite-temperature critical point and a $T_C = 0$ quantum critical point (QCP) cannot be reached. On the other hand, a recent study indicates that Rh substitution (hole doping) results in a continuous suppression of magnetism in the alloy $CePd_{1-x}Rh_x$, at $x \approx 0.87$ [18]. By studying the $x-p-T$ magnetic phase diagram of such alloys, it might be possible to identify for the first time a QCP on a ferromagnetic Ce system.

We selected $CePd_{0.6}Rh_{0.4}$ to perform the high-pressure multiprobe measurements presented here. Single crystals of this particular composition can be grown by Bridgman pulling technique [19]. Furthermore, the sharpness of the magnetic transition in $C_P(T)$ measurements at $T_C \approx 5.3$ K [20] hints that disorder-induced smearing is not strong at this concentration. Electrical current and T gradient were applied along the c-axis.

The electrical resistivity of $CePd_{0.6}Rh_{0.4}$ is plotted in Fig. 2. At low pressures, $p\sim0$, there is a characteristic maximum in the non-phononic resistivity $\rho_{mag} = \rho - \rho_{phonon} \approx \rho - 0.08\,\mathrm{T}$ at $T_\rho^{HT}\sim100$ K, represented by a ▼ on the $\rho(T)$ curve. This maximum results from crystal-field (CEF) effects on a Kondo system, and basically give a rough estimation of the total splitting Δ_{CEF} within the $J = \frac{5}{2}$ ground-state multiplet of Ce [21]. With increasing pressure, the maximum first shifts to lower temperature and it is no longer resolved for $4\,\mathrm{GPa} < p \leq 7.3$ GPa. But above 7.3 GPa, $T_\rho^{HT}(p)$ increases

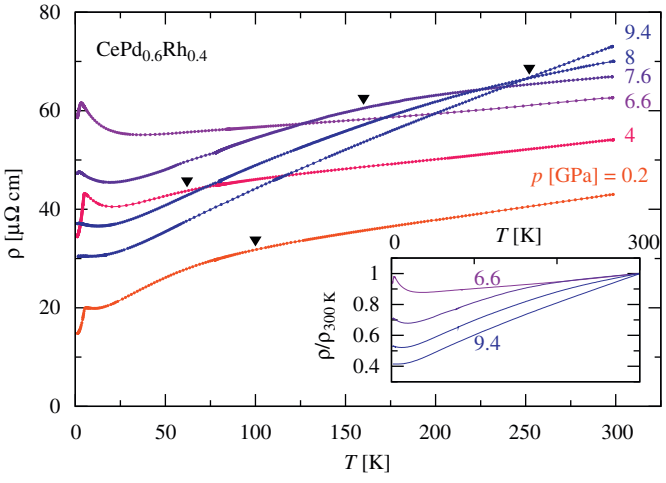

Fig. 2. Electrical resistivity of $CePd_{0.6}Rh_{0.4}$ at selected pressures. The full triangles (▼) signal the position of maxima in $\rho_{mag} = \rho - \rho_{phonon}$. The inset displays the $\rho(T)$ data normalized at 300 K, between 6.6 and 9.4 GPa. Notice the similarities between the p-variation of $\rho(T)$ in this alloy with the x-variation observed in $CePd_{1-x}Rh_x$ for $x \gtrsim 0.6$ (Ref. [18, Fig. 4]).

steeply from $T_\rho^{HT} \approx 160$ K at 7.6 GPa to $T_\rho^{HT} > 300$ K at 8.5 GPa, hinting that the Kondo temperature T_K increases drastically exceeding the crystal-field splitting in this pressure regime. A sharp valence crossover seems to occur around $p_v \approx 7.5$ GPa in a very narrow p-regime comparable to the pressure distribution in the cell.

At first sight, the overall $S(T,p)$-evolution depicted in Fig. 3 coincides with that of many Ce systems in which magnetism is suppressed through pressure or alloying, inducing an intermediate-valent state [6]. In view of the discussion of the previous paragraph, it is an advantage to extract the changes of characteristic temperatures from the thermopower because one does not have to deal with a (rather approximative) phonon substraction. One can see, however, that the same conclusion holds if the variation of $T_S^{HT}(p)$, indicated with ▽ in Fig. 3, is considered. That is, for pressures $p > 6.6$ GPa $T_K \sim T_S^{HT}$ rises steeply above room temperature which is again consistent with a valence change at $p_v \approx 7.5$ GPa.

The $T < 10$ K electrical resistivity is presented in Fig. 4 as $\Delta\rho \equiv \rho - \rho_0$ vs. T, in a log–log representation. At the lowest measured pressure, $p \approx 0.2$ GPa, the onset of ferromagnetism at $T_C(0) \approx 5.1$ K is accompanied by a sudden change of slope. The Curie temperature increases slightly with p, displaying a shallow maximum at $T_C \approx 5.2$ K for $p \sim 2.1$ GPa. A sharp feature still signals $T_C \approx 4.3$ K at 5.5 GPa, but in a narrow range 5.5 GPa $< p <$ 6.6 GPa the magnetic anomaly broadens considerably, as observed in 6.6 and 7.3 GPa measurements. The broadening of the magnetic anomaly is also detected in the heat capacity measurements (not shown). Tentatively, we associated this change in the low-T $\rho(T)$ and $C(T)$ to a continuous modification of the magnetic order from long-range ferromagnetism to a short-range glass-like order above $p^* \sim 6$ GPa.

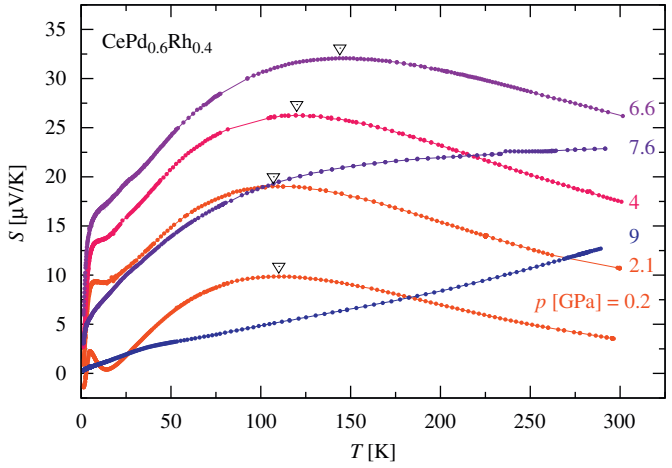

Fig. 3. Thermopower $S(T)$ of $CePd_{0.6}Rh_{0.4}$ at selected pressures. The measured p-variation roughly matches the expected evolution of a Ce-system from magnetic to intermediate valent [6]. The structure observed at low temperatures is related to magnetism, see the text for further details.

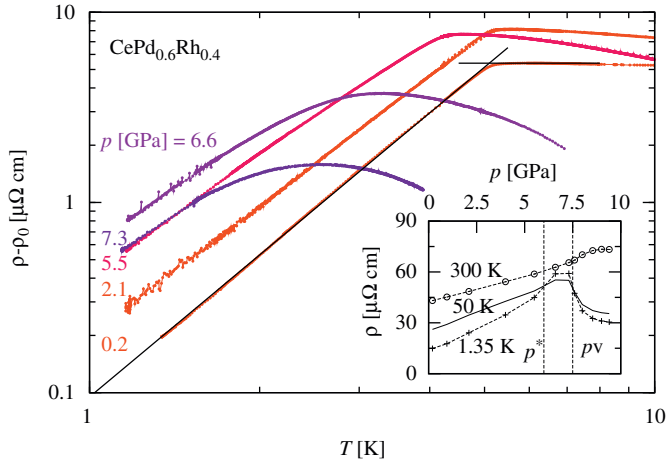

Fig. 4. Electrical resistivity of $CePd_{0.6}Rh_{0.4}$ plotted as $\Delta\rho \equiv \rho - \rho_0$ vs. T, in a log–log representation. Two straight lines show the extrapolated behaviors used to determine $T_C(0.2\,\text{GPa}) \approx 5.1$ K. Inset: isothermal evolution of the resistivity plotted at three different temperatures. Two vertical lines signal p^* and p_v.

A broad anomaly is still detected in $\rho(T)$ even at 9.4 GPa (i.e. well within the IV-state of the metal) but with a reduced amplitude that merely exceeds the noise level of our measurement. Also a strong characteristic drop in $S(T)$ and a small increase in C_p/T towards low temperatures [22] is observed at 8.5 GPa, reminiscent to the measurements performed on the $CePd_{1-x}Rh_x$ on the CeRh limit. All this information from three different physical properties lead us to suggest that only a small fraction of Ce moments are involved in the anomalies at high pressures and thus, they should be compared to (spin, cluster, etc.) glass order. One would expect that for $p \gtrsim p_v$ a larger majority of Ce moments are completely (Kondo) compensated at low temperatures, and that a smaller fraction remain unscreened due to the different local environments of the Ce^{3+}-ions in the alloy. Such a scenario has been already discussed in Ref. [23]. The fact that even in the pure IV compound CeRh (comparable to $CePd_{0.6}Rh_{0.4}$ around 9 GPa) a slight upturn in $\rho(T)$ is observed below 15 K [18] confirms the important effect of minute amounts of free moments in the transport properties of this system.

The evolution of the residual resistivity $\rho_0(p) \approx \rho(1.35\,\text{K}, p)$, plotted with crosses (+) in the inset of Fig. 4, deserves further analysis. Four different mechanisms seem to be responsible for its variation: (i) There is a contribution dominated by the substitutional disorder induced by alloying which, according to Nordheim rule, is almost maximal for $CePd_{0.6}Rh_{0.4}$. The amount of "static" disorder is probably increasing smoothly with p, due to unavoidable strain inside the pressure cell. (ii) Kondo-impurity scattering dominates in this alloy at low temperatures. A large contribution to the residual resistivity is due to a disruption of the lattice. (iii) Ferromagnetic critical spin fluctuations [24], and (iv) valence fluctuations [25] are expected to enhance the scattering from defects as p approaches the FM-QCP or the valence crossover, respectively. The effect of critical spin fluctuations is probably not a main contribution since the $T_C \to 0$ QCP is not accessible in $CePd_{0.6}Rh_{0.4}$. However, valence fluctuations can induce a large enhancement of ρ_0 when the valence crossover is sharp as reported for pressurized $CePd_{0.6}Rh_{0.4}$. It has been suggested that this contribution is at the origin of a bell-shaped p-dependence of ρ_0 in $CeCu_2Si_2$ [9], which has a similarity with $\rho(1.35\,\text{K}, p)$ and $\rho(50\,\text{K}, p)$ data.

The evolution of the different characteristic temperatures of pressurized $CePd_{0.6}Rh_{0.4}$ are plotted in the phase diagram of Fig. 5. The main observation that we extract from our data is the existence of a sharp valence crossover around $p_v \sim 7.5$ GPa, represented in the figure by a vertical line. In $CePd_{0.6}Rh_{0.4}$ the overall CEF-splitting is $\Delta_{CEF} \approx 200$ K [20], so the drastic changes of T_ρ^{HT} and T_S^{HT} across this line signal a sudden increase in $T_K(p)$ above room temperature. Magnetism is weakly affected for pressures $p \lesssim 5.5$ GPa, but in a p-window around $p^* \approx 6$ GPa the magnetic anomaly broadens as it shifts to lower temperatures. The proximity between p^* and p_v leads us to suggest that such change is to be interpreted as a collapse of ferromagnetism. The magnetic signal that survives into the intermediate valence phase is probably related to short-range correlations, rather than

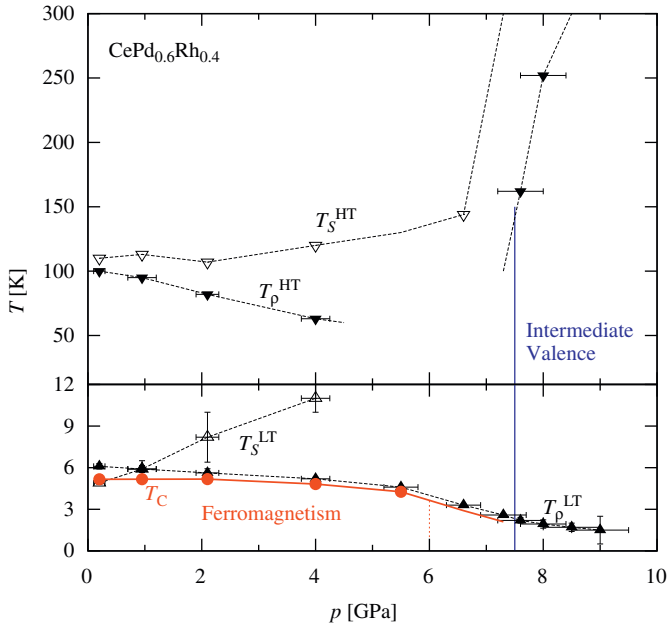

Fig. 5. Magnetic phase diagram of pressurized $CePd_{0.6}Rh_{0.4}$. Notice the change in the vertical scale at 12 K introduced in order to expand the low-T data.

long-range order. The question of the nature of the magnetic state for $p > p^*$ cannot be discussed using the techniques presented here.

4. Anomalous high-pressure transport properties of intermediate-valent $CePd_3$

On the Pd-rich side of the Ce–Pd binary system, $CePd_3$ is the first compound to display a non-magnetic ground state (Ce_3Pd_5 is ferromagnetic like CePd [3], while $CePd_5$ is also non-magnetic). This intermediate valence compound has a moderately enhanced Sommerfeld coefficient $\gamma = 38\,\mathrm{mJ/mol\,K^2}$ ($T_K \sim 600\,\mathrm{K}$) [26] but its electrical resistivity and thermopower are greatly augmented above the values found in other Ce-based IVC. Indeed, the low temperature $\rho(T) \sim AT^2$ Fermi-liquid coefficient, $A \approx 0.07\,\mu\Omega\,\mathrm{cm/K^2}$ [27,28], is almost an order of magnitude larger than $A \approx 0.01\,\mu\Omega\,\mathrm{cm/K^2}$ of the canonical $CeSn_3$ [29]. As a consequence, $CePd_3$ shares the "strongly correlated" branch of the Kadowaki–Woods plot with the heavy-fermion materials [29].

The published high-pressure resistivity data on $CePd_3$ [27,28,30] displays two notable features. First, results from experiments on powdered samples suggest that the resistivity maximum $T_\rho^m(p)$ has a non-monotonous evolution with p [30]. This result is surprising, since the Kondo temperature $T_K \sim 3T_\rho^m(p)$ [31] is expected to increase monotonously in Ce-systems. Second, the analysis of Lawrence et al. of the $T < T^* \sim 40\,\mathrm{K}$ resistivity suggests that $\rho(T)$ is almost unaffected by pressures up to 1.6 GPa [27], T^* being a characteristic scale different from T_K. The results of Ref. [28] seem to contradict this observation. In view of the listed controversial results, and the particular position of $CePd_3$ in the Kadowaki–Woods plot, we decided to perform simultaneous $\rho(T)$ and $S(T)$ measurements on a $CePd_3$ annealed polycrystal displaying a very low residual resistivity, $\rho_0 \approx 4.7\,\mu\Omega\,\mathrm{cm}$. This sample comes from the same batch as the one studied by Ref. [32].

In Fig. 6 we plot the measured resistivity as $\Delta\rho = \rho - \rho_0$ vs. T. These results were obtained at $p = 0$ and in two pressure runs up to 9.4 GPa (WC1, using WC-anvils) and 22.4 GPa (SD1, using sintered-diamond anvils). Two characteristics of the $\Delta\rho$ curves seem noteworthy: the first one is the weak pressure variation of

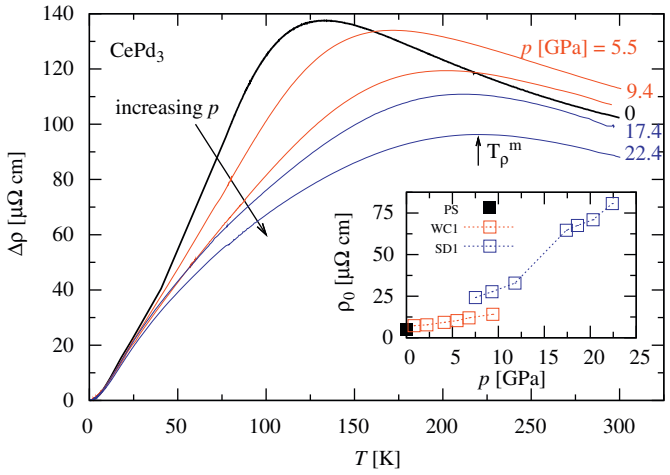

Fig. 6. Electrical resistivity of $CePd_3$ in a $\Delta\rho = \rho - \rho_0$ vs. T representation. The results from three different runs are included: PS labels the $p = 0$ measurement, WC1 was performed in a WC-anvil cell, while SD1 measurements where performed in a sintered-diamond anvil cell. Inset: the subtracted residual resistivity $\rho_0(p)$. The different variations of $\rho_0(p)$ suggest that the observed increase is mainly related to extrinsic (probably strain-induced) effects.

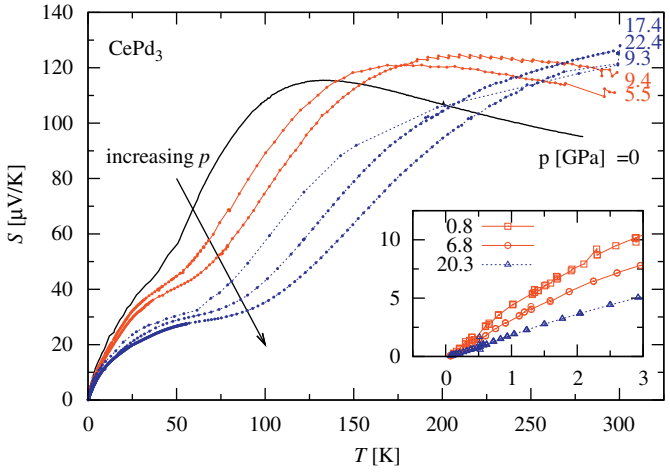

Fig. 7. Thermopower $S(T, p)$ of $CePd_3$ measured at $p = 0$ and high pressures. Notice the difference between the results measured in two different pressure cells (see the caption of Fig. 6) at $p \approx 9.3\,\mathrm{GPa}$. Inset: details of the low-T data showing the $S(T)$ measurements down to the mK range. Labels are the corresponding pressures in GPa.

the temperature of the resistivity maximum, $T_\rho^m(p)$, depicted in panel (a) of Fig. 8. The other is the fact that below $T \sim 30\,\mathrm{K}$ the resistivity of $CePd_3$ is practically unaffected by pressure. Further on, notice that the increasing $\rho_0(p)$ (see the inset of Fig. 6) and the fact that $CePd_3$ displays the so-called resistivity saturation [33], imply that $\Delta\rho(T)$ actually *underestimates* the variation of the resistivity.

At $p = 0$ our sample displays a $\Delta\rho = AT^n$ dependence with $n = 2$ between 1.5 and roughly 12 K, and a coefficient $A = 0.064\,\mu\Omega\,\mathrm{cm/K^2}$ within 12% of other values reported in the literature [27,28]. The resistivity data measured at high pressures do not deviate much from the $p = 0$ measurement and display basically the same temperature functionality, although with a lower exponent, $n \sim 1.7$. The origin of this T-dependence of $\rho(T)$ is not clear, since one would typically expect the zero pressure $\Delta\rho \propto T^2$ dependence to be maintained at high p. To simplify our analysis, we estimate a mean resistivity coefficient corresponding to the quadratic dependence as $A = \Delta\rho(10\,\mathrm{K})/100\,\mathrm{K^2}$, see panel (b) of Fig. 8.

The thermopower of $CePd_3$, see Fig. 7, is enhanced in the whole measured p range, in qualitative agreement with the resistivity results. There are, however, a few differences between the evolution of both transport properties, in particular, that of $T_S^m(p)$ in comparison with $T_\rho^m(p)$. The temperature of the maximums observed in both properties coincide at $p=0$. However, see panel (a) of Fig. 8, $T_S^m(p)$ measured in the cell WC1 increases linearly up to 9 GPa while the $T_\rho^m(p)$ increase already shows a small negative curvature. The mismatch may be due to the already quoted difficulty in measuring very large thermopowers like the one observed in $CePd_3$, even at high pressure. This point can be verified by comparing the $S(T)$ measurements performed in the two different pressure cells, WC1 and SD1, at $p \approx 9.3$ GPa. We ascribe this difference between $S(T,p)$ on pieces of the same polycrystal to an artifact from the measurement, for which the correction procedure (see Section 2) fails partially in the case of the SD1-cell. The lowest-T $S(T,p)$ seems not to be largely affected by this experimental issue, as suggested by the monotonous evolution of $S(10\,K)/10\,K$ presented in panel (c) of Fig. 8. Furthermore, a similar conclusion is obtained if we analyze the $S(T)$ measurements performed down to the mK range that are depicted in the inset of Fig. 7. The possibility of performing such type of measurement are especially appealing, particularly in view of the expected relation between S and $\gamma = C/T$ in SCES [34].

In Fig. 8 we compile the evolution of the different parameters that we have discussed. Panel (a) depicts the evolution of T_ρ^m and T_S^m. A clear tendency to saturation is observed in the $T_\rho^m(p)$ data.

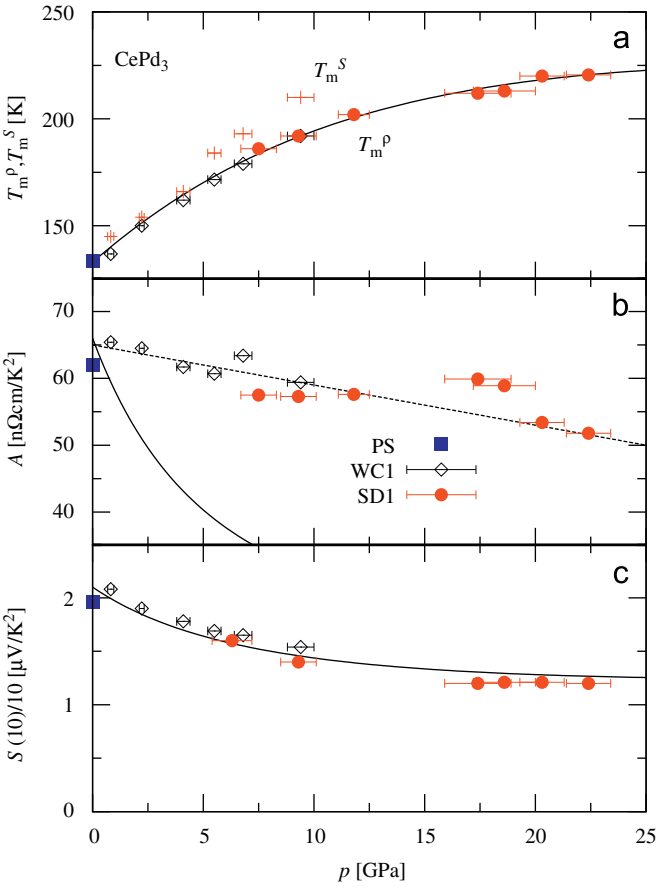

Fig. 8. Pressure evolution of parameters T_ρ^m, T_S^m, A and $S(10\,K)/10\,K$ for $CePd_3$. The full lines are described in the text. The dotted line of panel (b) is a linear fit to the data.

This could be an artifact related to increasing impurity scattering. However, a comparison with the results from doping studies [33] seems to indicate that the saturation of $T_\rho^m(p)$ is too strong in view of the ρ_0 increase. By assuming the validity of the relation $T_\rho^m \propto T_K$ and using the unit-cell volume variation at high pressures [28], we have estimated the Grüneisen parameter $\Gamma(p)$ for $CePd_3$ following the procedure of Ref. [35]. The full line in panel (a) represents the fitting to T_ρ^m, with $\Gamma(0) \approx 7.6$ and $\Gamma(22\,GPa) \sim 2$. This $\Gamma(0)$ value is expected for an IVC [1], but $\Gamma \sim 2$ is extremely small for a Ce system. Further on, the relations in a Kondo-lattice system $T_\rho^m \sim 1/\gamma \sim 1/\sqrt{A} \sim T/S$ allow us to compare in panels (b) and (c) the measured (symbols) and expected (full lines) evolutions of A and $S(10\,K)/10\,K$. While the description of $S(10\,K)/10\,K$ vs. p is quite satisfactory, the measured change of $A(p)$ is much weaker than $(1/T_\rho^m)^2$. These results point to a puzzling physical picture in which two energy scales extracted from $\rho(T)$ evolve only weakly under pressure and in a different manner. Preliminary band calculations fail to show a qualitative different picture between the responses of $CePd_3$ and isostructural $CeIn_3$ to pressure [36].

5. Conclusions

We have presented the results of multiprobe high-pressure experiments performed on two intermetallic Ce systems. The results on pressurized $CePd_{0.6}Rh_{0.4}$ indicate that ferromagnetism is weakly affected for $p \leq 5.5$ GPa, but strong changes are observed as $p \to p_v \approx 7.5$ GPa. At the pressure p_v we observe a drastic variation of several parameters, consistent with a sharp valence crossover of the Ce-state. In spite of the different initial behaviors of T_C under pressure, $dT_C/dp|_{p=0} > 0$, and doping, $dT_C/dx'|_{p=0} < 0$, the suppression of magnetism of $CePd_{0.6}Rh_{0.4}$ under p is very similar to that of $CePd_{0.6-x'}Rh_{0.4+x'}$ with increasing x' [18,23]. The proximity of p^* and p_v (equivalent to x^* and x_v in the alloy) indicates that the sudden delocalization of the 4f electron is what drives the collapse of long-range order into a state of short-range magnetic correlations. This latter state would not probably exist in stoichiometric α-CePd under pressure.

Surprisingly, $\rho(T)$ and $S(T)$ of $CePd_3$ change only weakly under applied pressure despite the estimated volume reduction at 20 GPa is larger than 10% (the bulk modulus is $B \approx 110$ GPa). Smaller volume contractions are typically required to observe large modifications of $\rho(T,p)$ and $S(T,p)$, as seen e.g. in the case of $CePd_{0.6}Rh_{0.4}$. To our knowledge, only the IVC $YbAl_3$ shows a similar p independence of $\rho(T,p)$ in a comparable pressure range [37]. The other striking result measured on $CePd_3$ is the failure of the proportionality $A \sim (T_\rho^m)^2$ when considering the broad p range studied here. Even though $CePd_3$ seems to be a pathological case, these results are a motivation to study other IVC to higher pressures.

Acknowledgments

We acknowledge E. Agoritsa for performing the $p=0$ measurements on $CePd_3$ and N. Penin for his assistance during the X-ray characterization of this compound.

References

[1] J.D. Thompson, J.M. Lawrence, in: K.A. Gschneidner Jr., L. Eyring, G.H. Lander, G.R. Choppin (Eds.), Handbook on the Physics and Chemistry of Rare Earths, vol. 19, North-Holland, Amsterdam, 1994 (Chapter 133).
[2] G.R. Stewart, Rev. Modern Phys. 73 (2001) 797; G.R. Stewart, Rev. Modern Phys. 78 (2006) 743.
[3] J.P. Kappler, et al., J. Less Common Metals 111 (1985) 261.
[4] A. Demuer, et al., Ann. Phys. 13 (2004) 72.
[5] D. Jaccard, et al., Rev. High Pressure Sci. Technol. 7 (1998) 412.

[6] P. Link, et al., Phys. B 225 (1996) 45.
[7] H. Wilhelm, Adv. Solid State Phys. 43 (2003) 889.
[8] R. Lortz, et al., J. Phys. Condens. Matter 17 (2005) 4135.
[9] A.T. Holmes, et al., Phys. Rev. B 69 (2004) 024508.
[10] T. Nakanishi, et al., Rev. Sci. Instrum. 73 (2002) 1828;
E. Colombier, D. Braithwaite, Rev. Sci. Instrum. 78 (2007) 093903.
[11] A.S. Rüetschi, D. Jaccard, Rev. Sci. Instrum. 78 (2007) 123901.
[12] Less than 50 Ce compounds displaying a ferromagnetic ground-state of ordered 4f-moments have been reported in the literature; 20% of these compounds contain Pd as one of its constituents.
[13] M.J. Thornton, et al., J. Phys. Condens. Mater 10 (1998) 9485.
[14] J.G. Sereni, et al., Phys. Rev. B 48 (1993) 3747.
[15] J.P. Kappler, et al., Phys. B 230 (1997) 162.
[16] D. Gignoux, J.C. Gómez Sal, Phys. Rev. B 30 (1984) 3967.
[17] J.L. Larrea, et al., Phys. Rev. B 72 (2005) 035129.
[18] J.G. Sereni, et al., Phys. Rev. B 75 (2007) 024432.
[19] M. Deppe, et al., Phys. B 378 (2006) 96.
[20] S. Hartmann, et al., J. Optoelectron. Adv. Mater. 10 (2008) 1607.
[21] B. Cornut, B. Coqblin, Phys. Rev. B 5 (1972) 4541.
[22] P. Pedrazzini, et al., unpublished.
[23] A.P. Pikul, et al., J. Phys. Condens. Matter 18 (2006) L535.
[24] K. Miyake, O. Narikiyo, J. Phys. Soc. Japan 71 (2002) 867.
[25] K. Miyake, H. Maebashi, J. Phys. Soc. Japan 71 (2002) 1007.
[26] M.J. Besnus, et al., J. Phys. F Met. Phys. 13 (1983) 597.
[27] J. Lawrence, et al., Phys. Rev. Lett. 54 (1985) 2537.
[28] G. Oomi, et al., Phys. B 163 (1990) 405.
[29] K. Kadowaki, S.B. Woods, Solid State Comm. 58 (1986) 507 and references therein..
[30] J.M. Mignot, J. Wittig, in: J.S. Schilling, R.N. Shelton (Eds.), Physics of Solids under High Pressure, North-Holland, Amsterdam, 1981, p. 311.
[31] M. Lavagna, et al., J. Phys. F Met. Phys. 12 (1982) 745.
[32] H. Sthioul, et al., in: P. Wachter, H. Boppart (Eds.), Valence Instabilities, North-Holland, Amsterdam, 1982, p. 443.
[33] H. Schneider, D. Wohlleben, Z. Phys. B Condens. Matter 44 (1981) 193.
[34] K. Behnia, et al., J. Phys. Condens. Matter 16 (2004) 5187.
[35] T. Kagayama, et al., J. Phys. Soc. Japan 63 (1994) 3927.
[36] T. Jarlborg, private communication.
[37] E. Colombier, Ph.D. Thesis, Université Joseph Fourier, Grenoble, 2008.